

# ENTRANCE-CHANNEL EFFECTS IN THE FUSION OF NICKEL ISOTOPES AT NEAR-BARRIER ENERGIES \* \*\*

S. COURTIN<sup>a</sup>, F. HOELLINGER<sup>a</sup>, N. ROWLEY<sup>a</sup>, A. LOPEZ-MARTENS<sup>a</sup>,  
F. HANNACHI<sup>b</sup>, O. STEZOWSKI<sup>a</sup>, A.J. BOSTON<sup>c</sup>, P. DAGNALL<sup>d</sup>,  
J. DURELL<sup>d</sup>, C. FINCK<sup>a</sup>, B.J.-P. GALL<sup>a</sup>, B. HAAS<sup>a</sup>, F. HAAS<sup>a</sup>,  
J. LISLE<sup>d</sup>, A. LUNT<sup>c</sup>, J.-C. MERDINGER<sup>a</sup>, E.S. PAUL<sup>c</sup>, H.C. SCRAGGS<sup>c</sup>,  
B. VARLEY<sup>d</sup>, AND J.-P. VIVIEN<sup>a</sup>.

<sup>a</sup>Institut de Recherches Subatomiques, B.P. 28  
F-67037 Strasbourg CEDEX 02, France

<sup>b</sup>CSNSM, CNRS-IN2P3, F-91405 Orsay, France

<sup>c</sup>Department of Physics, University of Liverpool, Liverpool L69 3BX, U.K.

<sup>d</sup>Department of Physics and Astronomy, University of Manchester  
Manchester M13 9PL, U.K.

*(Received August 5, 1998)*

Nuclear fusion at energies close to the Coulomb barrier emphasises interesting features of the interplay between reaction mechanisms and nuclear structure [1]. Both static and dynamical deformations of the target and projectile give rise to a range of Coulomb barriers depending on the orientation of the colliding nuclei, in the case of a rotational target, or the induced dynamical deformation in the vibrational case. In the vibrational, and almost symmetric,  $^{58}\text{Ni}+^{60}\text{Ni}$  system, a well defined discrete barrier distribution has been found [2]. This distribution is explained by strong multi-phonon couplings between the colliding nuclei. This interpretation of the fusion data led us to predict that an experiment performed at several energies covering the barrier distribution could reveal previously unobserved features of the spin distribution, including a spin population of the evaporation residues up to about  $20 \hbar$ , even 5 MeV below the conventional Bass barrier. Fusion of  $^{58}\text{Ni}$  with  $^{60}\text{Ni}$  at three near and sub-barrier energies has been studied in Strasbourg with a  $^{58}\text{Ni}$  beam from the VIVITRON accelerator on thin  $^{60}\text{Ni}$  targets, leading to the  $^{118}\text{Ba}^*$  compound nucleus. The  $\gamma$ -rays of the evaporation residues were identified in the GAREL+ array. Proton-rich isotopes of I, Xe, Te and Sb were observed, some up to spins of  $30 \hbar$ . A study of the relative population of these nuclei is presented and compared with calculations which accounts for of the correct barrier distribution.

PACS numbers: 29.30.Kv, 25.70.gh, 25.60.Pj

---

\* Presented at the International Conference "Nuclear Physics Close to the Barrier", Warszawa, Poland, June 30–July 4, 1998.

\*\* The presentation of this paper was awarded the Leopold Kronenberg prize for a young speaker.

## 1. Introduction

Enhancements of sub-barrier fusion cross-sections, that cannot be described by one dimensional barrier penetration models have been successfully explained in terms of coupled-channel calculations. These calculations can include couplings to inelastic or transfer channels [6, 7] as well as dynamic or permanent deformations of the reacting nuclei [8, 9]. The determination of the fusion barrier distribution is a good way to discriminate between the couplings involved in such a reaction. A simple way to extract the barrier distribution  $D(B)$  from fusion data has been established by Rowley *et al.* [1]. They have shown that  $D(B)$  is proportionnal to the second derivative of the fusion cross-section times the energy. Very accurate data for  $\sigma_{fus}$  are required to deduce  $D(B)$  by a point-difference method. Cross-section measurements with typical errors of about 1% have recently been performed in systems like  $^{16}\text{O} + ^{144,148,154}\text{Sm}$  or  $^{186}\text{W}$  [2–4] and barrier distributions showing interesting structures have been theoretically investigated. They can be explained by the strong influence of phonon excitations and/or effects of quadrupole or hexadecapole deformations. Furthermore, a dramatic three-peak structure in the barrier distribution has been found experimentally for the  $^{58}\text{Ni} + ^{60}\text{Ni}$  system by Stefanini *et al.* [5]. This surprising structure has been interpreted in terms of multi-phonon excitations, right up to the four-phonon channel. It has been shown that three distinct barriers, each weighted differently, are necessary in a Wong type model [8] to fit the experimental data properly. The full coupled-channel fit is shown in figure 1.

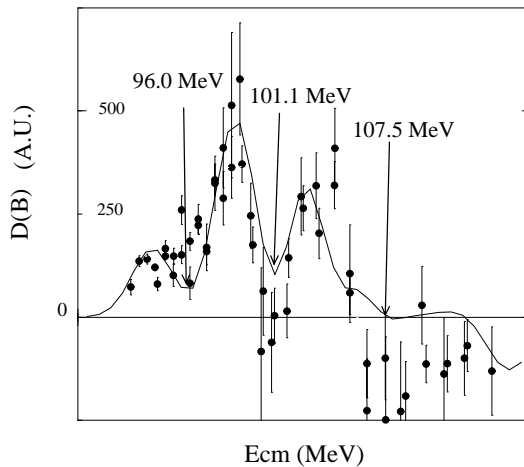


Fig. 1. Three-barrier fit of the experimental barrier distribution in  $^{58}\text{Ni} + ^{60}\text{Ni}$ , from Ref. [5]. The three energies of our study are indicated by arrows.

Very little is known about the influence of such reaction mechanisms on the structure of the populated nuclei. As the barrier distribution for  $^{58}\text{Ni} + ^{60}\text{Ni}$  is spread over more than 13 MeV, showing the most distinct structure known up to now, and as the fusion cross-section is known very accurately for this system, we chose this nearly symmetric system to study the influence of surface vibrations in the entrance channel on the population of the evaporation residues following near- and sub-barrier fusion.

## 2. Experiment

Three different bombarding energies just above the barriers, as shown in figure 1, have been chosen for our experiment. A  $^{58}\text{Ni}$  beam at 190.1 MeV, 199.9 MeV (mean barrier) and 212.3 MeV was successively delivered by the VIVITRON accelerator with a mean current of 10 pnA on  $^{60}\text{Ni}$  self-supporting targets. The target thicknesses were determined by alpha transmission and were  $252 \pm 25 \mu\text{g}\cdot\text{cm}^{-2}$  for the two lower energies and  $324 \pm 32 \mu\text{g}\cdot\text{cm}^{-2}$  for the highest one. The energy loss in the targets was thus kept below 3 MeV. The gamma-rays from the evaporation residues were identified in 13 large-volume germanium detectors of the GAREL+ array. A LEPS (Low-Energy Photon Spectrometer) detector was also mounted on the array to enhance the efficiency and resolution for low-energy transitions. The absolute efficiency for the set of Ge detectors was  $1.1 \pm 0.2 \%$ . Events were written to tape when at least 2 unsuppressed Ge detectors fired in prompt coincidence. The beam current was integrated at the beam dump in order to obtain the charge accumulated at each energy. The same system had already been studied at a higher energy (about 50 MeV above the barrier) to search for intruder bands in iodine isotopes [10]. Extensive level schemes of the principal evaporation residues of our study are known from this experiment. We could thus identify the strong  $3p$  channel,  $^{115}\text{I}$ , the  $2p$   $^{116}\text{Xe}$  channel, the  $(3p,2n)$   $^{113}\text{I}$ , the  $^{112}\text{Te}$  ( $(4p,2n)$  channel) and the  $^{115}\text{Xe}$  ( $(2p,n)$  channel) at each energy step of the experiment. More exit channels were open at the highest energy (just above the barrier), so that we could identify the low lying transitions in  $^{109}\text{Sb}$  ( $(5p,4n)$  channel) and  $^{114}\text{I}$  ( $(3p,n)$  channel). The region reached in this sub-barrier study is not far from the proton drip-line.

## 3. Results

Gamma-gamma matrices have been constructed for each energy and the statistics accumulated at the highest energy allowed us to build a cube. The part of the level schemes of the principal residues observed in the experiment is shown in figure 2.

The cross-sections for the observed evaporation residues were determined using  $\gamma$ -ray transitions. We have put some gates on the lowest transitions

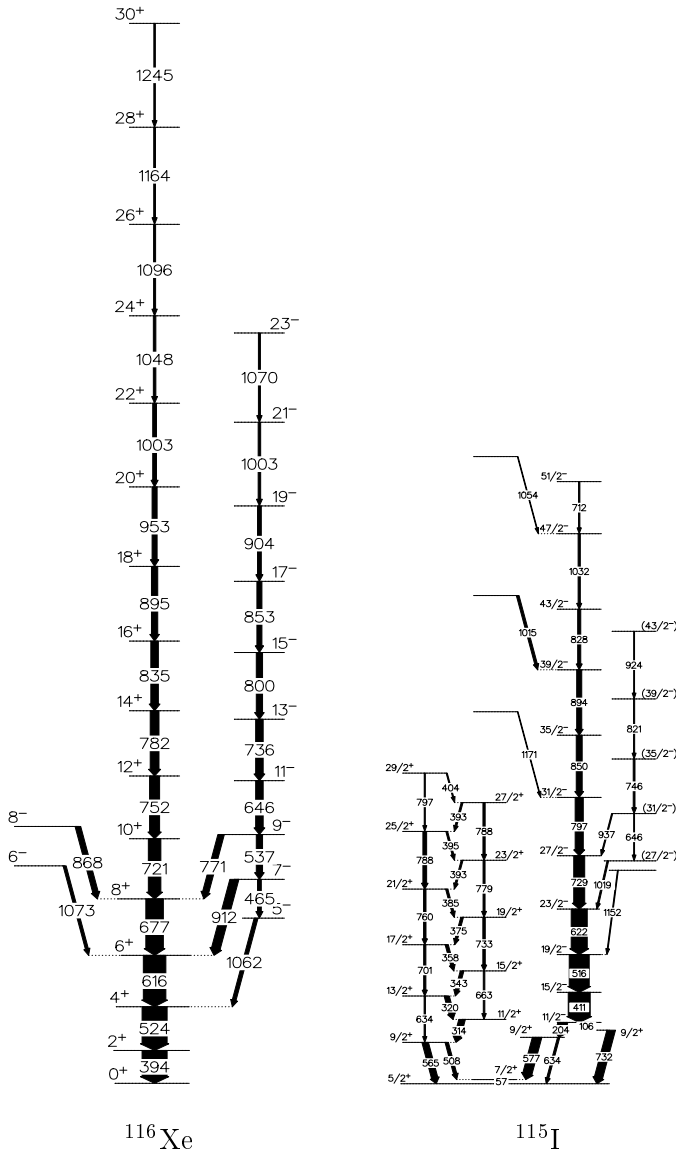


Fig. 2. Part of the level schemes of  $^{116}\text{Xe}$  and  $^{115}\text{I}$  observed in the present study.

of each residue and integrated the transitions falling onto the gated ones. The result was converted into cross-sections using the integrated charge. We have assumed that the feeding of the first states of the nuclei was negligible. This is corroborated by our study of the side-feeding of the residues (see

below). Contamination of the gates was avoided as much as possible and no long-life isomeric transitions are known in the nuclei studied. In  $^{116}\text{Xe}$ , the 1017 keV transition was not intense and the energy gate used is the  $(2^+ \rightarrow 0^+)$  394 keV transition. The case of this 3p channel ( $^{115}\text{I}$ ) is a little more complicated. The ground -state is populated via 4 transitions ( $(\frac{7}{2}^+ \rightarrow \frac{5}{2}^+)$  57 keV,  $(\frac{9}{2}^+ \rightarrow \frac{5}{2}^+)$  565 keV,  $(\frac{9}{2}^+ \rightarrow \frac{5}{2}^+)$  634 keV and  $(\frac{9}{2}^+ \rightarrow \frac{5}{2}^+)$  732 keV). We first chose the 411 keV, the 314 keV and the 634 keV transitions (see figure 2) to determine the cross-section for this channel. We tried estimating the cross-section using the lowest transitions but the accuracy of such a method is strongly affected by the accumulation of errors on the corrections for the efficiency. The same method was used for all the nuclei observed. A summary of the results is shown in Table I.

TABLE I

Experimental cross-sections (mb) of the principal residues observed. The errors are about 20%

Channel E <sub>beam</sub> (MeV)	$^{115}\text{I}$ 3p	$^{116}\text{Xe}$ 2p	$^{112}\text{Te}$ 4p,2n	$^{114}\text{Te}$ 4p	$^{113}\text{I}$ 3p,2n	$^{115}\text{Xe}$ 2p,n	$^{112}\text{I}$ 3p,2n	$^{114}\text{I}$ 3p,n
190.1	2.3	3.4	0.2	-	0.14	0.3	-	-
199.9	21.9	11.5	7.3	14.2	1.6	3.4	0.6	-
212.3	52.7	12.7	26.8	10.6	1.8	20.0	0.5	12.0

The spin population of the principal channels was estimated using the known  $\gamma$ -ray spectra. The side-feeding of each spin was obtained by subtracting the counts from transitions depopulating a spin from the ones populating this spin. Some results for the estimated spin population are presented in figure 3.

#### 4. Discussion

We have chosen the present reaction since the fusion cross-section was known to high precision and extremely well explained in terms of coupled-channel calculations. This allowed us a calculation of the entrance-channel spin distribution with some confidence, enabling us to draw conclusions on the evolution from the initial compound-nucleus configuration to the observed discrete  $\gamma$ -rays in the evaporation residues. In addition, the three distinct barriers observed in  $\sigma_{\text{fusion}}$  are known to correspond to different dynamical deformations of the target and projectile at the point of fusion. We might therefore hope to see if these shapes affect the subsequent particle

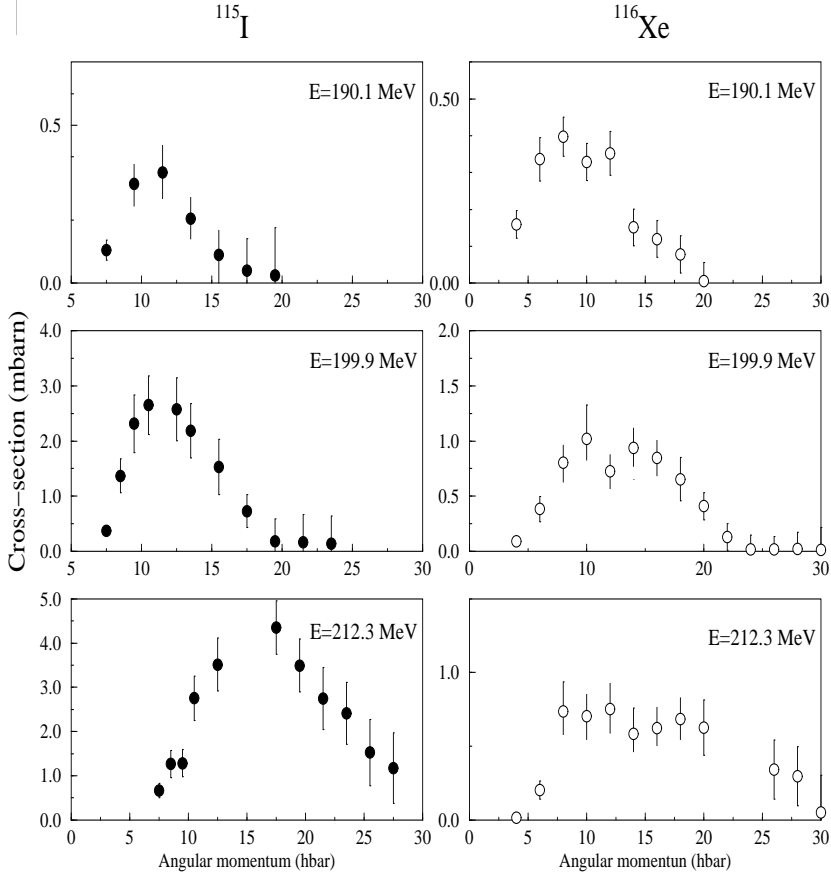


Fig. 3. Experimental spin distribution for the  $(2p,0n)$  and  $(3p,0n)$  channels at  $E_{\text{beam}} = 190.1$  MeV, 199.9 MeV and 212.3 MeV.

evaporation. The calculated spin distributions have structures reflecting the different fusion barriers as can be seen in figure 4. For  $E_{\text{beam}} = 199.9$  MeV, spins between 25 and 40  $\hbar$  are uniquely populated by a configuration in which the target and projectile both have a prolate deformation along their line of centres. This shape configuration is the only one leading to fusion for  $E_{\text{beam}} = 190.1$  MeV.

The results given by the EVAP computer code are in good agreement for the total fusion cross-section. Differences are observed for the  $2p$  and  $3p$  channels only for energies below the barrier. Moreover, for the second energy, we have observed a 14.2 mb  $4p$  channel ( $^{114}\text{Te}$ ) which was predicted by the code with only 0.3 mb. The Coulomb barrier is lowered for deformed nuclei, thus a deformation of the compound nucleus could be an explanation

TABLE II  
Fraction of the experimental cross-section for residues formed by (Xp,0n) emission.

$E_{\text{beam}}$ (MeV)	experiment	simulation
190.1	0.9	0.69
199.9	0.8	0.57
212.3	0.5	0.55

for the enhancement of proton emission at these energies as it is indicated in Table II. This is not observed at the last energy, which is above the Coulomb barrier (107.7 MeV) where effects of structure in the barrier tend to be averaged out.

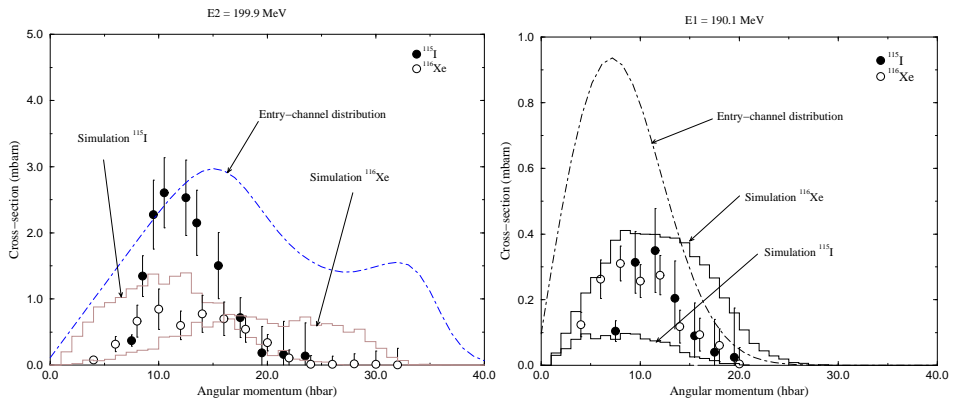


Fig. 4. Experimental and simulated spin distributions at 199.9 MeV and 190.1 MeV. The dot-dashed curves are the calculated compound nucleus distributions.

Figure 4, shows that states with spins between 20 and 30  $\hbar$  are not strongly fed in the experiment whereas it is predicted by the statistical-model code. Nevertheless the last transitions of  $^{115}\text{I}$  indicate that higher states could be populated. The behaviour of this nucleus, as many in this region has been interpreted in terms of band terminations [13]. The presence of non collective structures in this spin region would be an explanation for not observing yrast transitions above 25  $\hbar$ . It is of interest to notice that the shapes of the experimental distributions and their maxima are not very different for the two lowest energies in our study (see Fig. 3) even though 15  $\hbar$  more are brought in the system between  $E_1$  and  $E_2$ . On the other hand a clear enhancement is observed for the last energy, which might indicate that more collective structures may be present above the yrast line at higher spins.

We are indebted to Mr. Jean Devin for his valuable technical assistance throughout the experiment. We would also like to acknowledge the VIVITRON staff for the good conditions under which this experiment was performed.

## REFERENCES

- [1] N. Rowley, G. R. Satchler, P. H. Stelson, *Phys. Lett.* **B254**, 25 (1991).
- [2] J.R. Leigh *et al.*, *Phys. Rev.* **C47**, R437 (1993).
- [3] R.C. Lemmon *et al.*, *Phys. Lett.* **B316**, 32 (1993).
- [4] C.R. Morton *et al.*, *Phys. Rev. Lett.* **72**, 4074 (1994).
- [5] A.M. Stefanini *et al.*, *Phys. Rev. Lett.* **74**, 864 (1995).
- [6] C.H. Dasso *et al.*, *Nucl. Phys.* **A405**, 381 (1983).
- [7] R.A. Broglia *et al.*, *Phys. Lett.* **B133**, 134 (1983).
- [8] C.Y. Wong *et al.*, *Phys. Rev. Lett.* **31**, 766 (1973).
- [9] R. Stockstad *et al.*, *Phys. Rev.* **C23**, 23 (1981).
- [10] E.S. Paul *et al.*, *J. Phys. G* **18**, 837 (1992).
- [11] J.M. Sears *et al.*, *Phys. Rev.* **C57**, 2991 (1998).
- [12] J.R. Beene, N.G. Nicolis, D.G. Sarantites, EVAP computer code (unpublished).
- [13] E.S. Paul *et al.*, *Phys. Rev.* **C50**, 741 (1994).